Solitary wave propagation and interactions for the Klein–Gordon–Zakharov equations in plasma physics

2009 J. Phys. A: Math. Theor. 42 085205

(http://iopscience.iop.org/1751-8121/42/8/085205)

IOP PUBLISHING JOURNAL OF PHYSICS A: MATHEMATICAL AND THEORETICAL

J. Phys. A: Math. Theor. **42** (2009) 085205 (17pp) doi:10.1088/1751-8113/42/8/085205

Solitary wave propagation and interactions for the Klein–Gordon–Zakharov equations in plasma physics

Jian Wang

Department of Mathematics, Shanghai Jiaotong University, Shanghai 200240, People's Republic of China
and
Division of Computational Science, E-Institute of Shanghai Universities, SJTU, Shanghai 200030, People's Republic of China

E-mail: wj3156@sjtu.edu.cn

Received 26 August 2008, in final form 19 December 2008
Published 2 February 2009
Online at stacks.iop.org/JPhysA/42/085205

Abstract

The purpose of this paper is to show the advantages that represent the use of multisymplectic numerical methods that preserve the discrete multisymplectic conservation law in the study of solitary wave propagation and interaction for the Klein–Gordon–Zakharov equations in plasma physics. Numerical results on simulating the propagation of a single solitary wave and the interaction of two solitary waves are reported to illustrate the efficiency of the presented method.

PACS numbers: 02.60.Cb, 45.20.Jj, 52.35.Mw

(Some figures in this article are in colour only in the electronic version)

1. Introduction

The Klein–Gordon–Zakharov equations (KGZE) describe the interaction between Langmuir waves and ion sound waves [1, 2]. It takes an important role in the investigation of the dynamics of strong Langmuir turbulence in plasma physics. The KGZE can be derived from the two-fluid Euler–Maxwell system (see [3, 4], for instance). After suitable scaling it becomes in a dimensionless scalar form

$$c^{-2}\partial_t^2\phi - \Delta\phi + c^2\phi + \phi\psi = 0, \qquad \lambda^{-2}\partial_t^2\psi - \Delta\psi = \Delta|\phi|^2, \tag{1}$$

where ϕ is the electric field, ψ is the density fluctuation of ions, c^2 is the plasma frequency, and λ is the ion sound speed.

Masmoudi and Nakanishi [5, 6] proved that in the high-frequency limit $c \to \infty$ the KGZE (1) reduce to the Zakharov system

$$2\mathrm{i}\partial_t u - \Delta u + \psi u = 0, \qquad \lambda^{-2}\partial_t^2\psi - \Delta\psi = \Delta|u|^2. \tag{2}$$

In fact, we can eliminate the diverging term $c^2\phi$ in (1) by changing $\phi = e^{ic^2t}u$ to obtain

$$c^{-2}\partial_t^2 u + 2i\partial_t u - \Delta u + \psi u = 0, \qquad \lambda^{-2}\partial_t^2\psi - \Delta\psi = \Delta|u|^2. \tag{3}$$

If we take the limit $c \to \infty$, we get the usual Zakharov system (2). Further, in the simultaneous high-frequency and subsonic limits $c \to \infty, \lambda \to \infty$, the system (1) reduces to the nonlinear Schrödinger equation (NLS)

$$2i\partial_t u - \Delta u - |u|^2 u = 0, \qquad \psi = -|u|^2. \tag{4}$$

This can be seen by setting $\lambda \to \infty$ and letting $\psi = -|u|^2$ in (2).

In this paper, we consider the following one-dimensional KGZE:

$$\partial_t^2\phi - \partial_x^2\phi + \phi + \phi\psi = 0, \qquad \partial_t^2\psi - \partial_x^2\psi = \partial_x^2|\phi|^2. \tag{5}$$

There are a number of works on the qualitative research of the global solutions for the KGZE (5) problem in the literature (see [8–10], for details). Chen [11] considered orbital stability of solitary waves for the KGZE (5). Zhao and Sheng [12] obtained explicit traveling wave solutions of the KGZE with the aid of the symbolic computation system. More recently, Shang *et al* [13] used the extended hyperbolic functions method for analytic treatment for the KGZE and obtained the multiple exact explicit solutions. Specifically, Shang *et al* derived the following bell-type solitary wave solutions for the KGZE:

$$\begin{aligned}
\phi(x,t) &= \pm\sqrt{\frac{2(k^2-w^2+1+C)(k^2-w^2)}{-w^2}}\,\mathrm{sech}\left[\sqrt{\frac{(k^2-w^2+C+1)}{w^2-k^2}}(\xi+\xi_1)\right]e^{i(kx+wt+\xi_0)},\\
\psi(x,t) &= C - 2(k^2-w^2+C+1)\mathrm{sech}^2\left[\sqrt{\frac{(k^2-w^2+C+1)}{w^2-k^2}}(\xi+\xi_1)\right],
\end{aligned} \tag{6}$$

where k, w, C, ξ_0 and ξ_1 are arbitrary constants, $\xi = wx + kt$, and $(k^2 - w^2 + C + 1)(w^2 - k^2) > 0$.

The previous works mentioned above mostly focused on the approach to obtaining the analytic solutions and the stability of the analytic solution. Qualitative investigation on solutions is still insufficient, especially in studying the interaction of solitary waves. Therefore, developing numerical methods as well as setting up numerical experiments for this class of problems is highly important. However, up to now, few numerical methods and simulations have been proposed for the KGZE. In [14], Wang *et al* presented conservative difference methods for the KGZE.

As we know, the KGZE have similar shape to the Zakharov system. For the Zakharov system, many numerical methods and numerical simulations have been reported. Previous numerical studies include Fourier spectral methods [15], time-splitting spectral methods [16, 17], conservative finite difference schemes [18–20], etc. Thus, it is of great interest to develop an efficient, accurate numerical method for the KGZE.

In recent years, interest has grown rapidly in the Hamiltonian partial differential equations. Bridges and Reich presented the concept of the multisymplectic integrator based on a multisymplectic structure of some Hamiltonian PDEs such as the NLS and Klein–Gordon equations [21, 22, 24]. Subsequently, the multisymplectic methods and the conservation laws of several PDEs, such as the NLS [23, 27–29, 31, 32], the Zakharov system [33] and so on were discussed to obtain their solutions numerically. A great deal of numerical experiments and theory analysis show the advantages of the multisymplectic integrators in the structure, in the local conservation property and in the long-time simulating capability.

The NLS equations and the Zakharov system are typical model equations for plasma waves as well as other dispersive phenomena in physics. Recently, an upsurge of interest in

the analytic solution as well as the numerical methods for these equations has arisen (see [7] and references therein). However, the schemes used in [7] are not multisymplectic integrators.

To the best of our knowledge, there have been no studies on the multisymplecticity of the KGZE. In this paper, we will show that the KGZE (5) is a multisymplectic Hamiltonian system. As an application of this result, we will construct a multisymplectic pseudospectral scheme for solving the KGZE (5) with periodic boundary conditions

$$\begin{aligned} &\phi|_{t=0} = \phi_0(x), \quad \phi_t|_{t=0} = \phi_1(x), \quad \psi|_{t=0} = \psi_0(x), \quad \psi_t|_{t=0} = \psi_1(x), \\ &\phi(x_L, t)| = \phi(x_R, t), \quad \psi(x_L, t)| = \psi(x_R, t), \end{aligned} \tag{7}$$

where, $\phi_0(x)$, $\phi_1(x)$, $\psi_0(x)$ and $\psi_1(x)$ are given initial values.

The remainder of this paper is divided into four sections. In section 2, the multisymplectic formulation and some conservation laws for the KGZE (5) are discussed. Section 3 is concerned with multisymplectic Fourier pseudospectral discretizations for the KGZE (5). Numerical experiments are given in section 4. We perform the numerical simulations of propagation and head-on collision of solitary waves. Finally, some conclusions are contained in section 5.

2. Multisymplectic formulation and conservation laws for the KGZE

A partial differential equation $F(u, u_t, u_x, u_{tx}, \ldots) = 0$ is said to be multisymplectic if it can be written as a system of first-order equations (8):

$$\mathbf{M}\partial_t \mathbf{z} + \mathbf{K}\partial_x \mathbf{z} = \nabla_z S(\mathbf{z}), \tag{8}$$

where, $\mathbf{M}, \mathbf{K} \in \mathcal{R}^{d\times d}$ are skew symmetric, $\mathbf{z}(x, t)$ is the vector of state variables, $S : \mathcal{R}^d \to \mathcal{R}^1$ is a smooth function, and $\nabla_z S(\mathbf{z})$ denotes the gradient of the function $S = S(\mathbf{z})$ with respect to variable $\mathbf{z}$.

The multisymplectic formulation (8) is interesting for several reasons; one perhaps is the existence of the multisymplectic conservation law

$$\partial_t \omega + \partial_x \kappa = 0, \tag{9}$$

where ω and κ are pre-symplectic forms:

$$\omega = \tfrac{1}{2}\, \mathrm{d}\mathbf{z} \wedge \mathbf{M}\, \mathrm{d}\mathbf{z}, \qquad \text{and} \qquad \kappa = \tfrac{1}{2}\, \mathrm{d}\mathbf{z} \wedge \mathbf{K}\, \mathrm{d}\mathbf{z}, \tag{10}$$

which define a symplectic spacetime structure. The multisymplectic structure naturally gives rise to local conservation laws typically associated with Nöther's theorem [21]. In fact, for the Hamiltonian PDEs (8), when S is independent of x and t, it has local energy conservation law and local momentum conservation law:

$$\partial_t E + \partial_x F = 0, \qquad E = S(\mathbf{z}) - \tfrac{1}{2}\mathbf{z}^T \mathbf{K}\mathbf{z}_x, \qquad F = \tfrac{1}{2}\mathbf{z}^T \mathbf{K}\mathbf{z}_t, \tag{11}$$

$$\partial_t I + \partial_x G = 0, \qquad I = \tfrac{1}{2}\mathbf{z}^T \mathbf{M}\mathbf{z}_x, \qquad G = S(\mathbf{z}) - \tfrac{1}{2}\mathbf{z}^T \mathbf{M}\mathbf{z}_t. \tag{12}$$

For periodic or vanishing at infinity boundary conditions for the functions $F(\mathbf{z})$ and $G(\mathbf{z})$, one can obtain the global conservation laws of energy and momentum:

$$\frac{\mathrm{d}}{\mathrm{d}t}\mathcal{E}(z) = 0, \qquad \frac{\mathrm{d}}{\mathrm{d}t}\mathcal{I}(z) = 0, \tag{13}$$

where

$$\mathcal{E}(z) = \int_{\mathcal{R}} E(z(x, t))\, \mathrm{d}x \qquad \text{and} \qquad \mathcal{I}(z) = \int_{\mathcal{R}} I(z(x, t))\, \mathrm{d}x.$$

We call a numerical algorithm for (8) a multisymplectic algorithm if it preserves a discrete version of (9). For details, see [22–24], for instance.

In order to multisymplectify the KGZE (5), we set $\phi = u+\mathrm{i}v$, $\partial_x u = p$, $\partial_x v = q$, $\partial_t u = r$, $\partial_t v = s$, $\partial_t \psi = \partial_x^2 f$, $\partial_x f = g$ and $\mathbf{z} = (u, v, r, s, p, q, \psi, f, g)^T$. Then, the system (5) can be rewritten as the following first-order system:

$$\begin{aligned}
&-\partial_t r + \partial_x p = u + u\psi,\\
&-\partial_t s + \partial_x q = v + v\psi,\\
&\partial_t u = r,\\
&\partial_t v = s,\\
&-\partial_x u = -p,\\
&-\partial_x v = -q,\\
&\tfrac{1}{2}\partial_t f = \tfrac{1}{2}\psi,\\
&-\tfrac{1}{2}\partial_t \psi + \tfrac{1}{2}\partial_x g = 0,\\
&-\tfrac{1}{2}\partial_x f = -\tfrac{1}{2}g,
\end{aligned} \tag{14}$$

or the standard Hamiltonian PDEs (8) with the two skew-symmetric matrices

$$\mathbf{M} = \begin{pmatrix}
0 & 0 & -1 & 0 & 0 & 0 & 0 & 0 & 0\\
0 & 0 & 0 & -1 & 0 & 0 & 0 & 0 & 0\\
1 & 0 & 0 & 0 & 0 & 0 & 0 & 0 & 0\\
0 & 1 & 0 & 0 & 0 & 0 & 0 & 0 & 0\\
0 & 0 & 0 & 0 & 0 & 0 & 0 & 0 & 0\\
0 & 0 & 0 & 0 & 0 & 0 & 0 & 0 & 0\\
0 & 0 & 0 & 0 & 0 & 0 & 0 & \frac{1}{2} & 0\\
0 & 0 & 0 & 0 & 0 & 0 & -\frac{1}{2} & 0 & 0\\
0 & 0 & 0 & 0 & 0 & 0 & 0 & 0 & 0
\end{pmatrix},$$

$$\mathbf{K} = \begin{pmatrix}
0 & 0 & 0 & 0 & 1 & 0 & 0 & 0 & 0\\
0 & 0 & 0 & 0 & 0 & 1 & 0 & 0 & 0\\
0 & 0 & 0 & 0 & 0 & 0 & 0 & 0 & 0\\
0 & 0 & 0 & 0 & 0 & 0 & 0 & 0 & 0\\
-1 & 0 & 0 & 0 & 0 & 0 & 0 & 0 & 0\\
0 & -1 & 0 & 0 & 0 & 0 & 0 & 0 & 0\\
0 & 0 & 0 & 0 & 0 & 0 & 0 & 0 & 0\\
0 & 0 & 0 & 0 & 0 & 0 & 0 & 0 & \frac{1}{2}\\
0 & 0 & 0 & 0 & 0 & 0 & 0 & -\frac{1}{2} & 0
\end{pmatrix}.$$

The right-hand side of (8) is then given by the gradient of the scalar function

$$S(\mathbf{z}) = \tfrac{1}{2}(u^2+v^2) + \tfrac{1}{2}(u^2+v^2)\psi + \tfrac{1}{2}(r^2+s^2) - \tfrac{1}{2}(p^2+q^2) + \tfrac{1}{4}\psi^2 - \tfrac{1}{4}g^2.$$

A straightforward calculation shows that the system (14) satisfies the multisymplectic conservation law:

$$\frac{\partial}{\partial t}\left(\mathrm{d}r\wedge\mathrm{d}u + \mathrm{d}s\wedge\mathrm{d}v + \frac{1}{2}\,\mathrm{d}\psi\wedge\mathrm{d}f\right) + \frac{\partial}{\partial x}\left(\mathrm{d}u\wedge\mathrm{d}p + \mathrm{d}v\wedge\mathrm{d}q + \frac{1}{2}\,\mathrm{d}f\wedge\mathrm{d}g\right) = 0. \tag{15}$$

The density functions defined in (11)and (12) are given by

$$\begin{aligned}
E &= \tfrac{1}{2}(u^2+v^2)+\tfrac{1}{2}\psi(u^2+v^2)+\tfrac{1}{2}(p^2+q^2)+\tfrac{1}{2}(r^2+s^2)+\tfrac{1}{4}(\psi^2+g^2),\\
F &= -\big(u_t p + v_t q + \tfrac{1}{2} f_t g\big),\\
I &= u_x r + v_x s - \tfrac{1}{2}\psi_x f,\\
G &= \tfrac{1}{2}(u^2+v^2)+\tfrac{1}{2}\psi(u^2+v^2)-\tfrac{1}{2}(p^2+q^2+r^2+s^2)+\tfrac{1}{4}(\psi^2-g^2)+\tfrac{1}{2}\psi_t f.
\end{aligned} \tag{16}$$

Integrating E and I over the spatial domain with periodic or vanishing at infinity boundary conditions leads to the global conservation of energy and momentum (13), where

$$\begin{aligned}
\mathcal{E} &= \int_{\mathcal{R}} \left(|\phi_t|^2 + |\phi_x|^2 + |\phi|^2 + \psi|\phi|^2 + \frac{1}{2}|g|^2 + \frac{1}{2}|\psi|^2 \right) \mathrm{d}x,\\
\mathcal{I} &= \int_{\mathcal{R}} \left[\Re(\phi_x \bar{\phi}_t) - \frac{1}{2}\psi_x f \right] \mathrm{d}x.
\end{aligned} \tag{17}$$

These are two important global conservative quantities for the KGZE (5).

3. Multisymplectic pseudospectral discretization of the KGZE

The Fourier transforms can leave the multisymplectic nature of a PDE unchanged, and that the discretized Fourier system recovers the standard spectral discretizations leading to a system of Hamiltonian ODEs which can be integrated by standard symplectic integrators [24, 27].

We consider a uniform spatial grid. Let $\Lambda = [x_L, x_R]$ and $L = x_R - x_L$. The interval Λ is divided into N equal subintervals with the grid spacing $h = L/N$, where the integer N is even. The spatial grid points are given by $x_j = x_L + hj$, $j = 0, 1, \ldots, N-1$. We denote by $u_j, v_j, p_j, q_j, \psi_j, f_j, g_j$ the approximation to $u(x_j,t), v(x_j,t), p(x_j,t), q(x_j,t), \psi(x_j,t), f(x_j,t), g(x_j,t)$, respectively, and introduce the notation

$$\begin{aligned}
&\mathbf{u} = (u_0, u_1, \ldots, u_{N-1})^T, \quad \mathbf{v} = (v_0, v_1, \ldots, v_{N-1})^T, \quad \mathbf{p} = (p_0, p_1, \ldots, p_{N-1})^T,\\
&\mathbf{q} = (q_0, q_1, \ldots, q_{N-1})^T, \quad \mathbf{f} = (f_0, f_1, \ldots, f_{N-1})^T, \quad \mathbf{g} = (g_0, g_1, \ldots, g_{N-1})^T.
\end{aligned} \tag{18}$$

By applying the Fourier pseudospectral method to equations (14) and using the first-order Fourier pseudospectral differential matrix D_1, we obtain

$$\begin{aligned}
&-\frac{\mathrm{d}}{\mathrm{d}t} r_j + (D_1 \mathbf{p})_j = u_j + u_j \phi_j,\\
&-\frac{\mathrm{d}}{\mathrm{d}t} s_j + (D_1 \mathbf{p})_j = v_j + v_j \phi_j,\\
&\frac{\mathrm{d}}{\mathrm{d}t} u_j = r_j,\\
&\frac{\mathrm{d}}{\mathrm{d}t} v_j = s_j,\\
&(D_1 \mathbf{u})_j = p_j,\\
&(D_1 \mathbf{v})_j = q_j,\\
&\frac{\mathrm{d}}{\mathrm{d}t} f_j = \big(u_j^2 + v_j^2\big) + \psi_j,\\
&-\frac{\mathrm{d}}{\mathrm{d}t} \psi_j + (D_1 \mathbf{g})_j = 0,\\
&(D_1 \mathbf{f})_j = g_j.
\end{aligned} \tag{19}$$

The elements of D_1 are

$$d_{j,s} = \begin{cases} (-1)^{j+s}\dfrac{\pi}{L}\cot\dfrac{(x_j - x_s)\pi}{L}, & s \neq j, \\ 0, & s = j. \end{cases}$$

Note that D_1 is a skew-symmetric matrix.

From the computational point of view, the evaluation of the pseudospectral Fourier derivatives is computed by using the FFT algorithm instead of spectral differentiation matrix in $\mathcal{O}(N \log N)$ operations rather than $\mathcal{O}(N^2)$.

Using the similar calculations in [27, 31], we can obtain the following semi-discrete multisymplectic conservation laws:

$$\frac{\mathrm{d}}{\mathrm{d}t}\omega_j + \sum_{k=0}^{N-1} d_{jk}\kappa_{jk} = 0, \qquad (j = 0, 1, \ldots, N-1), \tag{20}$$

where

$$\begin{aligned} &\omega_j = \mathrm{d}r_j \wedge \mathrm{d}u_j + \mathrm{d}s \wedge \mathrm{d}v_j + \tfrac{1}{2}\,\mathrm{d}\psi_j \wedge \mathrm{d}f_j, \\ &\kappa_{jk} = \mathrm{d}u_j \wedge \mathrm{d}p_k + \mathrm{d}v_j \wedge \mathrm{d}q_k + \tfrac{1}{2}\,\mathrm{d}f_j \wedge \mathrm{d}g_k + \mathrm{d}u_k \wedge \mathrm{d}p_j + \mathrm{d}v_k \wedge \mathrm{d}q_j + \tfrac{1}{2}\,\mathrm{d}f_k \wedge \mathrm{d}g_j, \end{aligned} \tag{21}$$

which is a spectral discretization of the multisymplectic conservation law (9). Thus the Fourier pseudospectral discretization preserves the multisymplectic structure of the PDEs (8).

The skew symmetry of D_1 provides the conservation of total symplecticity. Since $D_1^T = -D_1$ and $\kappa_{jk} = \kappa_{kj}$, summing over the spatial index, equation (20) becomes

$$\frac{\mathrm{d}}{\mathrm{d}t}\sum_{j=0}^{N-1}\omega_j = 0, \tag{22}$$

which implies the conservation of total symplecticity in time.

For the time discretization of (19), we use an implicit midpoint method for obtaining

$$\begin{aligned} &-\delta_t^+ r_j + (D_1\mathbf{p}^{n+1/2})_j = u_j^{n+1/2} + u_j^{n+1/2}\phi_j^{n+1/2}, \\ &-\delta_t^+ s_j + (D_1\mathbf{p}^{n+1/2})_j = v_j^{n+1/2} + v_j^{n+1/2}\phi_j^{n+1/2}, \\ &\delta_t^+ u_j = r_j^{n+1/2}, \\ &\delta_t^+ v_j = s_j^{n+1/2}, \\ &(D_1\mathbf{u}^{n+1/2})_j = p_j^{n+1/2}, \\ &(D_1\mathbf{v}^{n+1/2})_j = q_j^{n+1/2}, \\ &\delta_t^+ f_j = \left(u_j^{n+1/2}\right)^2 + \left(v_j^{n+1/2}\right)^2 + \psi_j^{n+1/2}, \\ &-\delta_t^+ \psi_j + (D_1\mathbf{g}^{n+1/2})_j = 0, \\ &(D_1\mathbf{f}^{n+1/2})_j = g_j^{n+1/2}, \end{aligned} \tag{23}$$

where δ_t^+ denotes the difference operator $\delta_t^+\mathbf{z}_j^n = \frac{1}{\Delta t}\left(\mathbf{z}_j^{n+1} - \mathbf{z}_j^n\right)$, $u_j^{n+1/2} = \frac{1}{2}\left(u_j^{n+1} + u_j^n\right)$ etc.

Rewriting (23) as the abstract form

$$\mathbf{M}\delta_t^+\mathbf{z}_j^n + \mathbf{K}\sum_{j=0}^{N-1} d_{jk}\mathbf{z}_k^{n+1/2} = \nabla_z S\left(\mathbf{z}_j^{n+1/2}\right), \tag{24}$$

it is now straightforward to show that the Fourier pseudospectral scheme (24) has N fully discrete multisymplectic conservation laws:

$$\delta_t^+ \omega_j^n + \sum_{k=0}^{N-1} d_{jk} \kappa_{jk}^{n+1/2} = 0, \qquad (j = 0, 1, \ldots, N-1), \tag{25}$$

where

$$\omega_j^n = \mathrm{d}r_j^n \wedge \mathrm{d}u_j^n + \mathrm{d}s_j^n \wedge \mathrm{d}v_j^n + \tfrac{1}{2}\,\mathrm{d}\psi_j^n \wedge \mathrm{d}f_j^n,$$
$$\kappa_{jk}^{n+1/2} = \mathrm{d}u_j^{n+1/2} \wedge \mathrm{d}p_k^{n+1/2} + \mathrm{d}v_j^{n+1/2} \wedge \mathrm{d}q_k^{n+1/2} + \tfrac{1}{2}\,\mathrm{d}f_j^{n+1/2} \wedge \mathrm{d}g_k^{n+1/2}$$
$$+ \mathrm{d}u_k^{n+1/2} \wedge \mathrm{d}p_j^{n+1/2} + \mathrm{d}v_k^{n+1/2} \wedge \mathrm{d}q_j^{n+1/2} + \tfrac{1}{2}\,\mathrm{d}f_k^{n+1/2} \wedge \mathrm{d}g_j^{n+1/2}.$$

Taking the summation of equation (25) over all spatial grid points and noting that

$$\sum_{j=0}^{N-1} \sum_{k=0}^{N-1} d_{jk} \kappa_{jk}^{n+1/2} = 0,$$

we can obtain the full-discrete symplectic conservation law

$$\sum_{j=0}^{N-1} \omega_j^{n+1} = \sum_{j=0}^{N-1} \omega_j^n.$$

4. Numerical experiments

According to [13], the KGZE has the bell-type analytic solitary wave solution (6). For simplicity, in our numerical experiments, we take $k = \nu$ and $\omega = \sqrt{\nu^2 + 0.5}$. Thus the KGZE (5) admits the following solitary wave solution:

$$\begin{aligned} \phi(x, t, \nu) &= \frac{1}{\sqrt{2\nu^2 + 1}} \operatorname{sech}(\sqrt{\nu^2 + 0.5}(x - x_0) + \nu t) \exp(\mathrm{i}(\nu(x - x_0) + \sqrt{\nu^2 + 0.5}t)) \\ \psi(x, t, \nu) &= -\operatorname{sech}^2(\sqrt{\nu^2 + 0.5}(x - x_0) + \nu t), \end{aligned} \tag{26}$$

where x_0 and ν are constants, and ν indicates the propagating velocity of solitary wave, x_0 is the initial phase. The amplitude of the ϕ component is $\frac{1}{\sqrt{2\nu^2+1}}$, while the amplitude of the ψ component is 1. In the following, our computations will work on the spatial domain $\left[-\frac{L}{2}, \frac{L}{2}\right]$, over the time interval $0 \leqslant t \leqslant T$ with constant time step length Δt and spatial step length $\Delta x = L/N$. Here N is the number of grid points for the spatial domain. We use periodic boundary conditions, i.e.,

$$\phi\left(-\frac{L}{2}, t\right) = \phi\left(\frac{L}{2}, t\right), \qquad \psi\left(-\frac{L}{2}, t\right) = \psi\left(\frac{L}{2}, t\right).$$

4.1. Travelling of single solitary wave

We begin our study by simulating the evolution of a single solitary wave to test the accuracy of the multisymplectic Fourier pseudospectral method. The initial values

$$\phi_0 = \phi(x - x_0, 0, \nu), \qquad \phi_1 = \phi_t(x - x_0, t, \nu)|_{t=0},$$
$$\psi_0 = \psi(x - x_0, 0, \nu), \qquad \psi_1 = \psi_t(x - x_0, t, \nu)|_{t=0}$$

are obtained from (26) as $t = 0$.

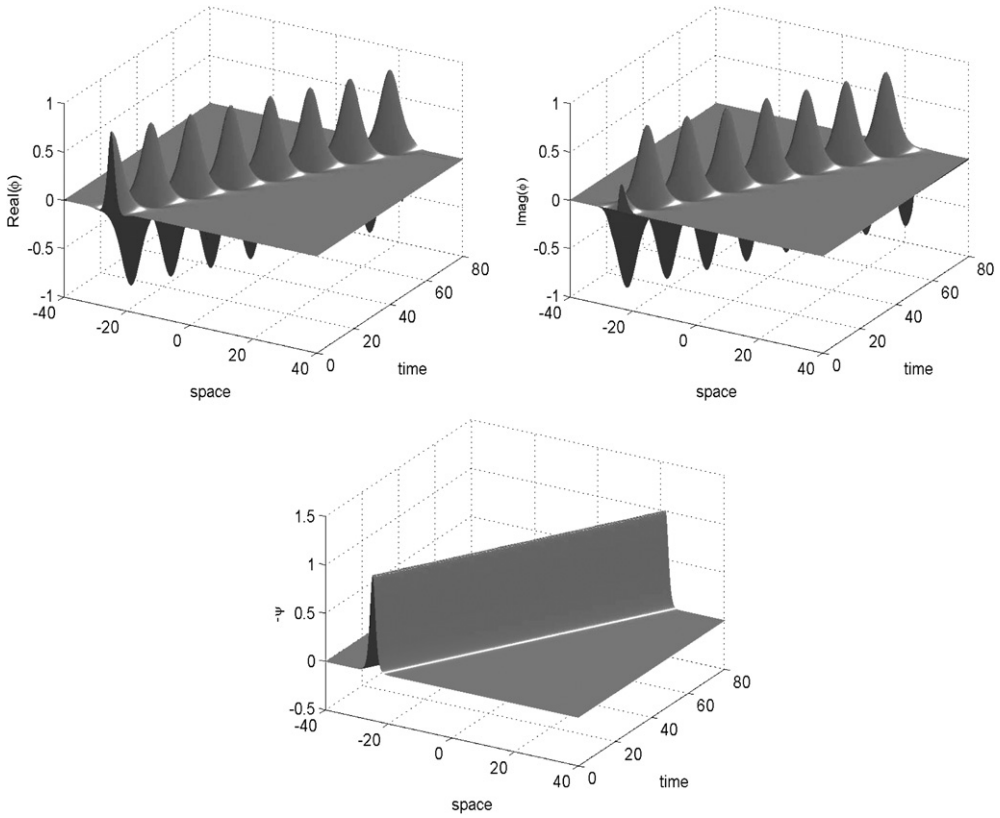

Figure 1. The evolution of numerical solutions. The real part (upper left) and imaginary part (upper right) of ψ and ψ (bottom), respectively, with $\Delta t = 0.02$ and $N = 512$.

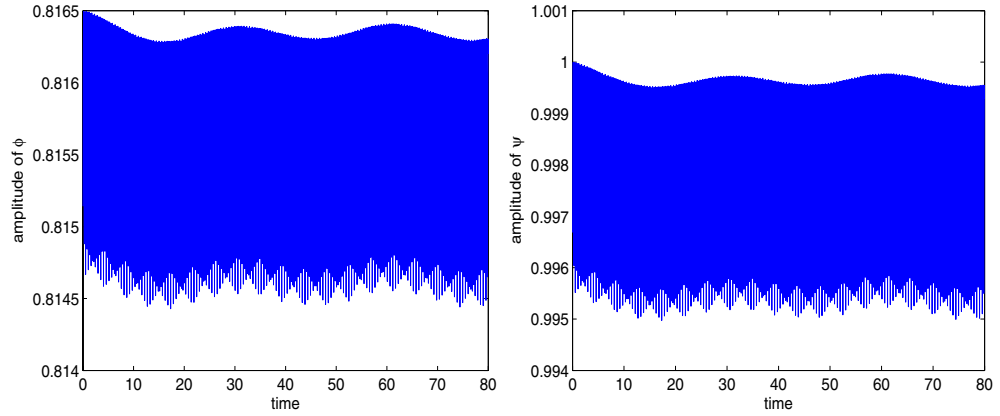

Figure 2. Amplitudes of solitary waves against time. Left plot: ϕ component, right plot: ψ component.

Figure 1 presents the evolution of the numerical solutions ϕ, ψ for the solitary wave in the time interval $[0, 80]$ with $\nu = 0.5, x_0 = -25, \Delta t = 0.02$ and $N = 512$. For the solitary wave solution (26), the wave amplitude of the ϕ component is about 0.816 497. In figure 2, the wave profile is plotted against time for two components of the KGZE. From the

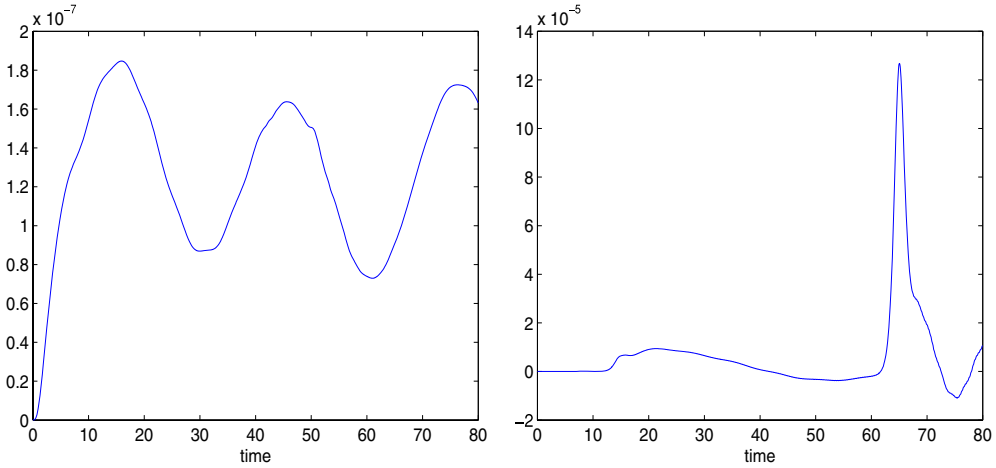

Figure 3. Global error of discrete conservation laws. Left plot: energy, right plot: momentum.

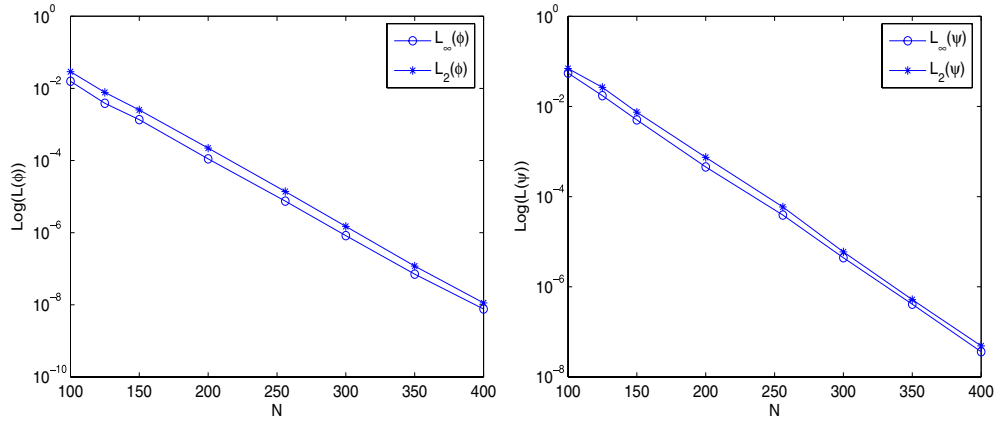

Figure 4. The convergence rate of the multisymplectic Fourier pseudospectral method in space: $\Delta t = 0.0001, T = 5$.

above results, we find that the waveforms keep their amplitudes and velocities near invariable throughout the processes of simulations, which implies that the present method can preserve the local properties of the travelling wave solution perfectly. Figure 3 shows the global energy and momentum conservations. We see that the global energy and momentum are bounded in long-time integration, and the scheme preserves the energy $\mathcal{E}$ and momentum $\mathcal{I}$ with the accuracy of 10^{-7} and 10^{-5} in the L_∞ norm, respectively. Thus, the method is stable in the sense of the energy and momentum conservation laws.

To test whether the present method exhibits the expected convergence rates in time and in space, we define the errors between numerical solutions and analytic solutions in the sense of L_2 and L_∞ norms as

$$\|L(\phi)\|_2 = \left(h \sum_{j=0}^{N-1} \left| \phi(x_j, t_n) - \phi_j^n \right|^2 \right)^{\frac{1}{2}}, \qquad \|L(\phi)\|_\infty = \max_{0 \leqslant j \leqslant N-1} \left| \phi(x_j, t_n) - \phi_j^n \right|, \tag{27}$$

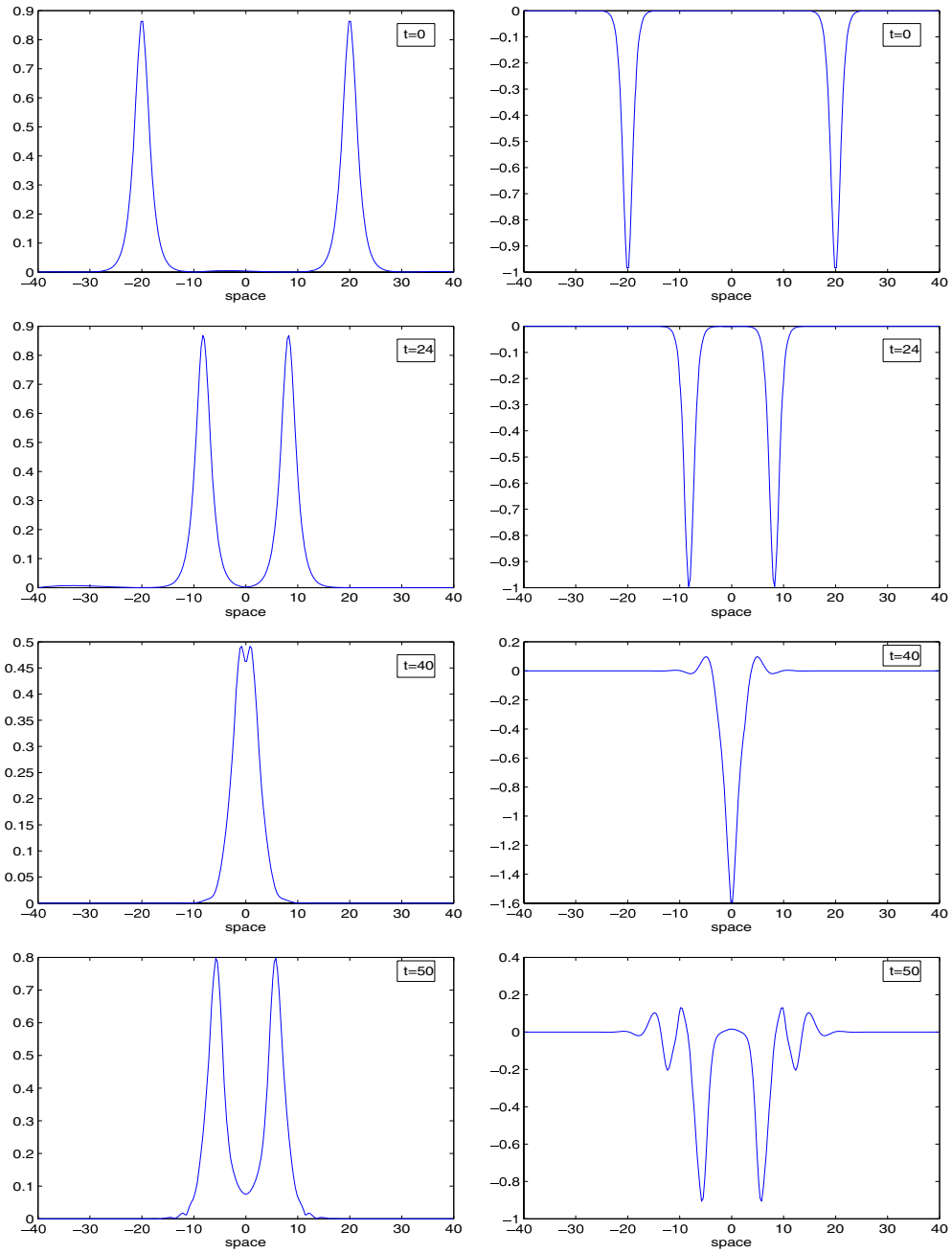

Figure 5. The collision of two solitary waves in case 1. Left plot: $|\phi|$, right plot: ψ.

$$\|L(\psi)\|_2 = \left(h \sum_{j=0}^{N-1} \left| \psi(x_j, t_n) - \psi_j^n \right|^2 \right)^{\frac{1}{2}}, \qquad \|L(\psi)\|_\infty = \max_{0 \leqslant j \leqslant N-1} \left| \psi(x_j, t_n) - \psi_j^n \right|. \quad (28)$$

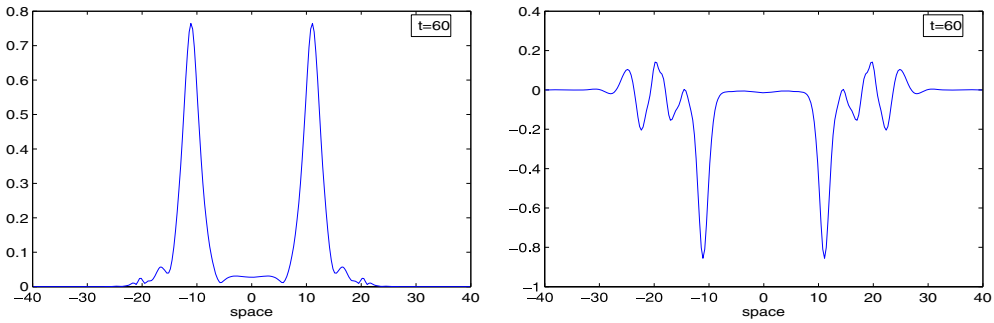

Figure 5. (Continued.)

Table 1. Accuracy of the multisymplectic Fourier pseudospectral method, $N = 256$, $T = 10$.

Δt	1.0×10^{-2}	5.0×10^{-3}	4.0×10^{-3}	3.0×10^{-3}	2.0×10^{-3}
$\|L(\phi)\|_\infty$	3.462×10^{-4}	2.164×10^{-5}	1.385×10^{-5}	7.789×10^{-6}	3.461×10^{-6}
Order	–	2.00	2.00	2.00	2.00
$\|L(\phi)\|_2$	5.416×10^{-4}	3.394×10^{-5}	2.179×10^{-5}	1.241×10^{-5}	5.895×10^{-6}
Order	–	2.00	2.00	2.00	2.00
$\|L(\psi)\|_\infty$	3.786×10^{-4}	2.361×10^{-5}	1.509×10^{-5}	8.498×10^{-6}	3.806×10^{-6}
Order	–	2.00	2.00	2.00	2.00
$\|L(\psi)\|_2$	4.922×10^{-4}	3.076×10^{-5}	1.965×10^{-5}	1.107×10^{-5}	4.922×10^{-6}
Order	–	2.00	2.00	2.00	2.00

Table 1 reports the errors between the exact solutions and the numerical solutions derived from the scheme (23), and the convergence order of accuracy in time. It can be seen that the scheme is of second-order accuracy in time.

To test whether the present method exhibits the expected convergence in space, we perform some further numerical experiments for various values of N and a fixed value of time step Δt. In these experiments, we take $\Delta t = 10^{-4}$ so that the time discretization error can be ignored compared to the spatial discretization error.

Figure 4 presents, in the logarithmic scale, the evolution in the space of the error of the numerical solution for the present method. One can see that the numerical solution converges rapidly to the accurate solution in the space, which is an indication of exponential convergence.

4.2. Collision of two solitary waves

In this subsection, two different head-on interaction cases are considered. In the first case, solitary waves of equal amplitude propagate at equal initial speed in opposite directions ($v_1 = -v_2 = 0.4$), and in the second case solitary waves of different amplitudes propagate at initial speeds ($v_1 = 0.4$ and $v_2 = -0.2$). The corresponding initial values are given as

$$\begin{aligned} \phi_0 &= \phi_l(x - x_l, 0, v) + \phi_r(x - x_r, 0, v), & \phi_1 &= [\phi_l(x - x_l, t, v) + \phi_r(x - x_r, t, v)]|_{t=0} \\ \psi_0 &= \psi_l(x - x_l, 0, v) + \psi_r(x - x_r, 0, v), & \psi_1 &= [\psi_l(x - x_l, t, v) + \psi_r(x - x_r, t, v)]|_{t=0}, \end{aligned} \tag{29}$$

where x_l, x_r are initial phases.

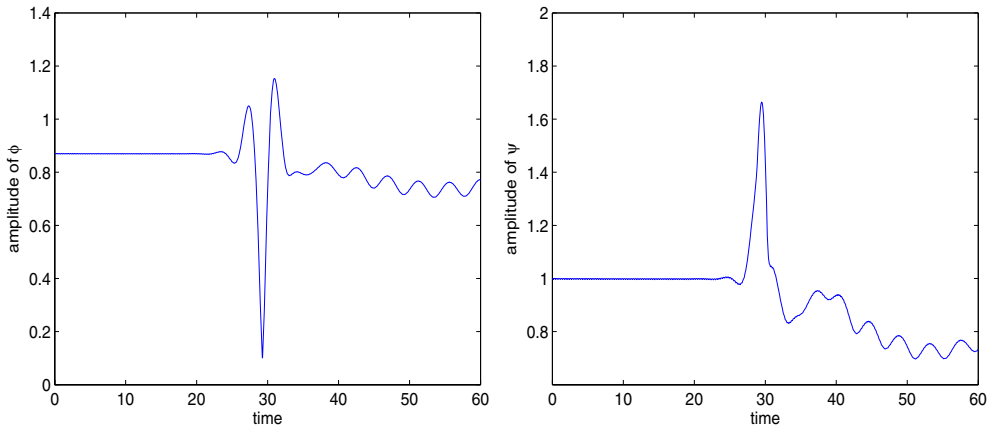

Figure 6. Amplitudes of solitary waves against time. Left plot: ϕ component, right plot: ψ component.

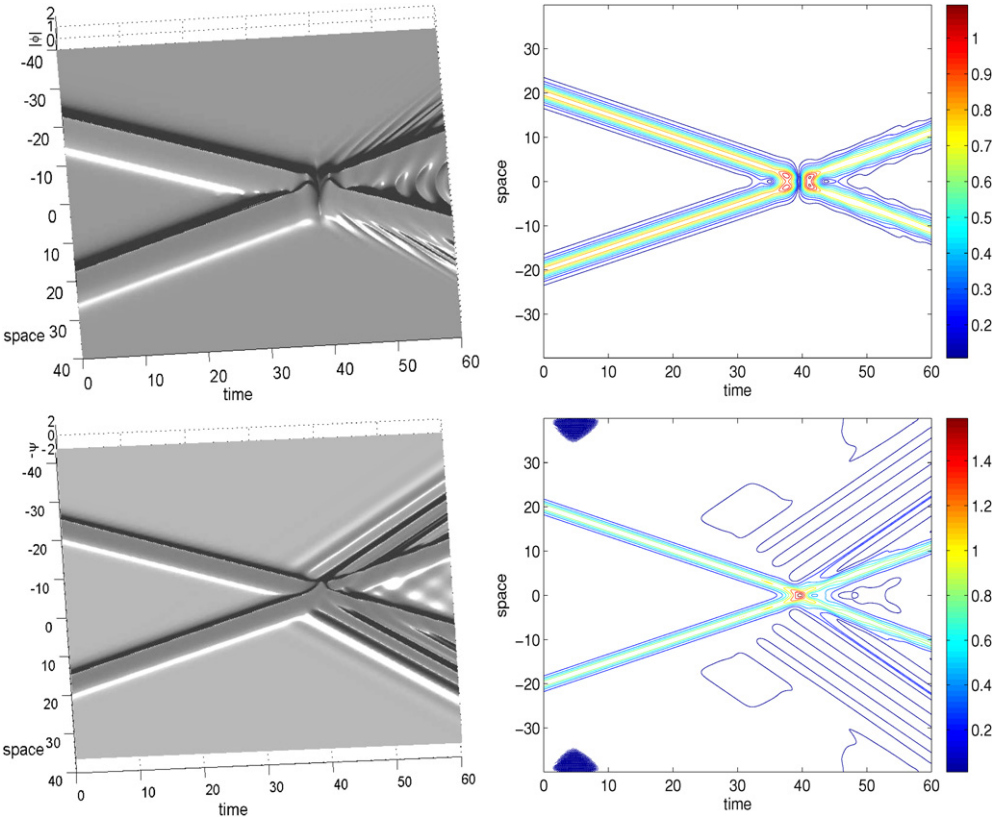

Figure 7. Collisions of two solitary waves in case 1. Top plot: $|\phi|$, bottom plot: $-\psi$.

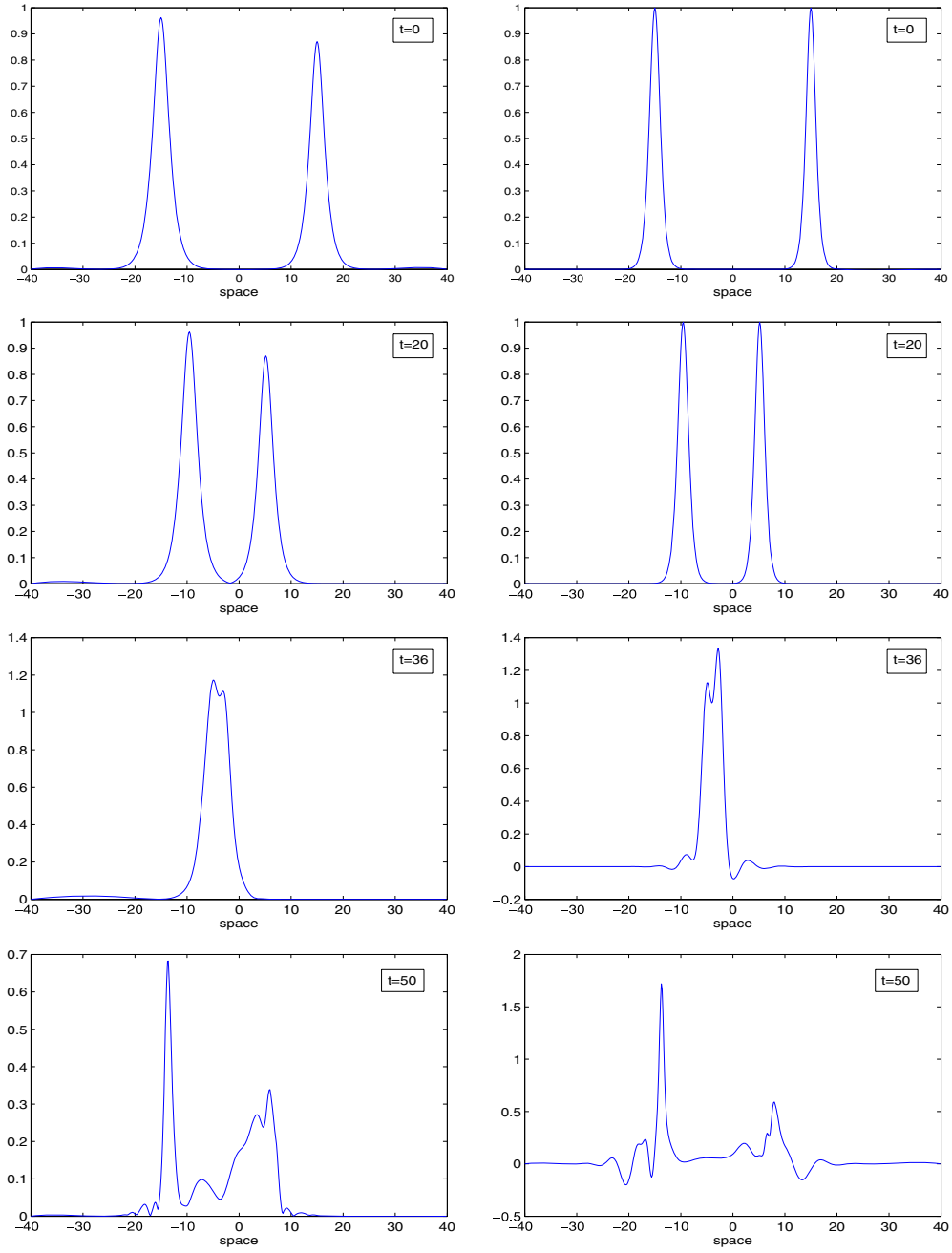

Figure 8. The collision of two solitary waves in case 2. Left plot: $|\phi|$, right plot $-\psi$.

Case 1: head-on collision of solitary waves with equal amplitudes.

In this case, the interaction between two solitary waves having initial velocities $v_l = -v_r = 0.4$ and initial phases $x_l = -x_r = -20$ is studied. Numerical integration is carried out for

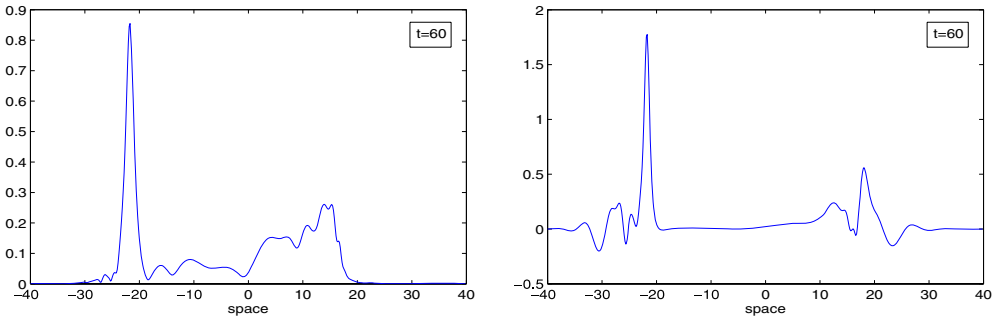

Figure 8. (Continued.)

$0 \leqslant t \leqslant 60$, time step length $\Delta t = 0.02$ and spatial step length $N = 512$. Two solitary waves of equal amplitude are placed along the x-axis: the one on the left is set moving in the right direction, while the other one on the right is moving in the left direction. Consequently, these two solitary waves will have a head-on collision later on. The resulting evolution of the solution is plotted against time in figure 5. It is clear from the pictures that after the collision solitary waves do not preserve themselves. Figure 6 shows the amplitude curves of the solutions. It is found that before the collision of the two solitary waves, the waveforms keep their amplitudes near invariable. However, after the collision, the amplitudes oscillate rapidly. The fact that amplitudes are not restored after interaction indicates that interactions between solitary waves are not elastic, i.e., a certain exchange of energy takes place between solitary waves during interaction. Figure 7 exhibits the graphs of three dimensions and contour plots of numerical solutions for the collision of two solitary waves in case 1. We can conclude that (1) the initial symmetric shape of solitary waves is preserved during the interaction, (2) for the ϕ component of the solution, after the interaction we observe an interaction of the dispersive tails following the two solitary waves as they separate and an enlargement of the ripples in front of them, and (3) for the ψ component of the solution, the initial solitary waves spawn a well-defined hierarchy of multiple secondary solitary waves.

Case 2: head-on collision of solitary waves with non-equal amplitudes.

In a similar manner, we discuss interaction of two solitary waves having initial velocities $v_l = 0.2$ and $v_r = -0.4$. The simulation of their temporal evolution was done on time interval $[0, 60]$ with $\Delta t = 0.02$ and $N = 512$. Case 2 corresponds to the collision of a right-going soliton with a larger peak value of amplitude and a left-going soliton with a smaller value of amplitude. The numerical solution for the collision process is plotted in figures 8 and 9. Figure 10 shows the amplitude curves of the solutions which implies that the collision between solitary waves is not elastic. From these pictures, we view that the features of the collision of solitary waves are basically the same as in the previous case. However, some differences are still observed: (1) for ϕ component of solitary waves, the amplitude of the lower solitary wave increases, whereas the high one decreases after interaction; (2) for ψ component of solitary waves, the amplitude of the left-going wave (with speed $v = 0.4$) increases while the amplitude of the right-going wave (with speed $v = 0.2$) decreases after interaction. This is an interesting phenomenon; and (3) phase shifts appear for both components of solitary waves during interaction.

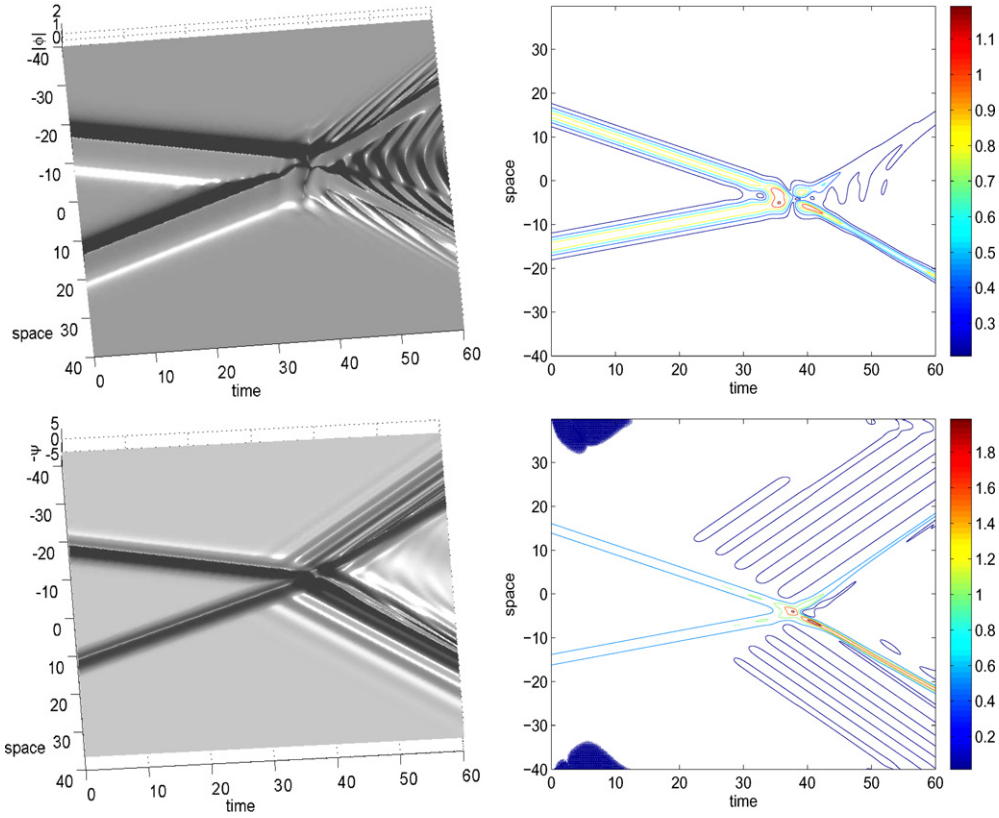

Figure 9. Collisions of two solitary waves in case 2. Top plot: $|\phi|$, bottom plot: $-\psi$.

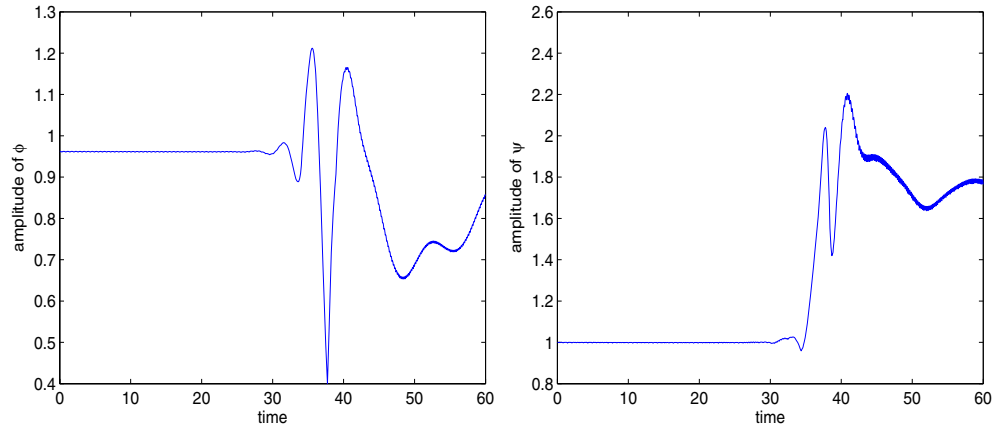

Figure 10. Amplitudes of solitary waves against time. Left plot: ϕ component, right plot: ψ component.

5. Conclusion

Numerical experiments in the study of the solitary wave dynamics is an important research approach, because the exact solution of nonlinear equations is generally unknown. This paper

studied the interaction of two solitary waves of the KGZE (5). We presented a multisymplectic formulation for the KGZE (5). Based on this formulation, we developed a multisymplectic pseudospectral method for discretizating the KGZE. The method is implicit, of spectral accuracy in space and second-order accuracy in time. Numerical experiments demonstrate the remarkable capacity of this method for simulating the propagation and the collision of the solitary waves in long-time integration.

Acknowledgments

The author would like to thank anonymous referees for their valuable suggestions. The author wishes to thank Shenqi Wang for the part of numerical simulation. This work is supported by the National Natural Science Foundation of China (grant no 10871127) and E-Institutes of Shanghai Municipal Education Commission (grant no E03004).

References

[1] Thornhill S G and Haar D 1978 Langmuir turbulence and modulational instability *Phys. Rep.* **43** 43–99
[2] Dendy R O 1990 *Plasma Dynamicx* (Oxford: Oxford University Press)
[3] Colin M and Colin T 2004 On a quasilinear Zakharov system describing laser–plasma interactions *Differ. Integr. Equ.* **17** 297–330
[4] Texier B 2007 Derivation of the Zakharov equations *Arch. Ration. Mech. Anal.* **184** 121–83
[5] Masmoudi N and Nakanishi K 2005 From the Klein–Gordon–Zakharov system to the nonlinear Schröinger equation *J. Hyperbolic Differ. Equ.* **2** 975–1008
[6] Masmoudi N and Nakanishi K 2008 Energy convergence for singular limits of Zakharov type systems *Invent. Math.* **172** 535–83
[7] Belashov V Y and Vladimirov S V 2005 *Solitary Waves in Dispersive Complex Media* (Berlin: Springer)
[8] Guo B L and Yuan G W 1995 Global smooth solution for the Klein–Gordon–Zakharov equations *J. Math. Phys.* **36** 4119–24
[9] Tsutaya K 1996 Global existence of small amplitude solutions for the Klein–Gordon–Zakharov equation *Nonlinear Anal. Theory Methods Appl.* **27** 1373–80
[10] Adomian G 1997 Non-perturbative solution of the Klein–Gordon–zakharov equations *Appl. Math. Comput.* **81** 89–92
[11] Chen L 1999 Orbital stability of solitary waves for the Klein–Gordon–Zakharov equations *Acta Math. Applacatae Sin. (English Ser.)* **15** 54–64
[12] Zhao C H and Sheng Z M 2004 Explicit traveling wave solutions for Zakharov equation *Acta Phys. Sin.* **53** 1629–34 (in Chinese)
[13] Shang Y D, Huang Y and Yuan W J 2008 New exact traveling wave solutions for the Klein–Gordon–Zakharov equations *Comput. Math. Appl.* **56** 1441–50
[14] Wang T C, Chen J and Zhang L 2007 Conservative difference methods for the Klein–Gordon–Zakharov equations *J. Comput. Appl. math.* **205** 430–52
[15] Payne G L, Nicholson D R and Downie R M 1983 Numerical solution of the Zakharov system *J. Comput. Phys.* **50** 482–98
[16] Shi J, Markowich P A and Zheng C X 2004 Numerical simulation of a generalized Zakharov system *J. Comput. Phys.* **201** 376–95
[17] Bao W, Sun F F and Wei G W 2003 Numerical methods for the generalized Zakharov system *J. Comput. Phys.* **190** 201–28
[18] Chang Q and Jiang H 1994 A conservative difference scheme for the Zakharov equations *J. Comput. Phys.* **113** 309
[19] Chang Q and Jiang H 1995 Finite difference method for generalized Zakharov equations *Math. Comput.* **64** 537
[20] Glassey R 1992 Convergence of an energy-preserving scheme for the Zakharov equations in one space dimension *Math. Comput.* **58** 83
[21] Marsden J E, Patick G P and Shkoller S 1999 Multisymplectic geometry, variational integrators and nonlinear PDEs *Commun. Math. Phys.* **199** 351–95
[22] Bridges T J 1999 Multi-symplectic structures and wave propagation *Math. Proc. Camb. Phil. Soc.* **121** 147–90

[23] Bridges T J and Reich S 2001 Multi-symplectic integrators: numerical schemes for Hamiltonian PDEs that conserve symplecticity *Phys. Lett.* A **284** 184–93
[24] Bridges T J and Reich S 2001 Multi-symplectic spectral discretizations for the Zakharov–Kuznetsov and shallow water equations *Physica* D **152** 491–504
[25] Reich S 2000 Multi-symplectic Runge–Kutta collocation methods for Hamiltonian wave equation *J. Comput. Phys.* **157** 473–99
[26] Moore B and Reich S 2003 Multisymplectic integration methods for Hamiltonian PDEs *Future Gener. Comput. Syst.* **19** 395–402
[27] Chen J B and Qin M Z 2001 Multi-symplectic Fourier pseudospectral method for the nonlinear Schrödinger equation *Electron. Trans. Numer. Anal.* **12** 193–204
[28] Islas A L, Karpeev D A and Schober C M 2001 Geometric integrators for the nonlinear Schrödinger equation *J. Comput. Phys.* **173** 116–48
[29] Islas A L and Schober C M 2003 Multi-symplectic methods for generalized Schrödinger equations *Future Gener. Comput. Syst.* **19** 403–13
[30] Islas A L and Schober C M 2004 On the preservation of phase space structure under multi-symplectic discretization *J. Comput. Phys.* **197** 585–609
[31] Wang J 2007 Multisymplectic Fourier pseudospectral method for the nonlinear schrödinger equations with wave operator *J. Comput. Math.* **25** 31–48
[32] Wang J 2007 A note on multisymplectic Fourier pseudospectral method for the nonlinear Schrödinger equation *Appl. Math. Comput.* **191** 31–41
[33] Wang J 2008 Multisymplectic integrator of the Zakharov system *Chin. Phys. Lett.* **25** 3531–4